International Journal of Power and Energy Systems, Vol. 44, No. 10, 2024
An Open Access Paper

CAPACITY OPTIMISATION CONFIGURATION OF HYBRID ENERGY STORAGE SYSTEM CONSIDERING PRIMARY FREQUENCY REGULATION OUTPUT OF WIND FARM

Zhiye Lu,* Jinze Yu,* Liyang Sun,* Yupeng Xiong,* Bing Yang,* Ruolin Yin,* and Lishu Wang*

Abstract

The large-scale grid integration of renewable energy will lead to power system frequency stability problems, and grid primary frequency modulation demand problems are increasingly prominent. To improve the primary frequency modulation stability of wind energy storage systems and meet the primary frequency modulation output requirements of wind farms, this paper takes the minimisation of hybrid energy storage system (HESS) capacity allocation costs as the goal when the HESS meets the primary frequency modulation output requirements of wind farms in the power system, also considers the charging and discharging constraints, and adopts an artificial fish swarm algorithm with an improved moving strategy to select the optimal filtering number of the variational mode decomposition (VMD) to optimise the capacity allocation. Finally, the rationality of the proposed research method is verified by combining the 96-h historical data of wind farms in a certain area. After analysis, the following conclusions are drawn: the method can realise a reasonable allocation of hybrid energy storage capacity and, at the same time, meet the primary frequency modulation output demand of wind farms in the power system. In addition, by providing primary frequency modulation services, wind farms are able to obtain certain economic benefits. The significance of this study is to improve the stability of primary frequency modulation in wind farms by optimising the capacity configuration of the wind storage system, which in turn enhances the stability of the power system. It plays a key role in promoting the large-scale application of renewable energy and realising the energy transition, while also providing strong support for power system reliability and sustainable development.

* School of Electrical and Information, Northeast Agricultural University, Harbin 150030, China; e-mail: s221402006@neau.edu.cn
Corresponding author: Lishu Wang

(DOI: 10.2316/J.2024.203-0529)

Key Words

Hybrid energy storage, capacity optimisation, variational mode decomposition, wind power, primary frequency modulation

1. Introduction

In recent years, with the continuous economic growth and the continuous improvement of residents' living standards, the penetration rate of clean energy, such as wind and solar power generation is increasing [1], [2]. However, after the large-scale access of renewable energy to the power grid, the power generation side and the user side are prone to load imbalance, which affects the frequency stability of the power grid and seriously threatens the economic and safe operation of the power grid [3]. Traditional thermal power units are usually large in scale and slow in frequency regulation response. The frequent start and stop of the unit will cause energy waste and cause great damage to the unit [4]. There is an urgent need for effective technical solutions to solve the problem of grid frequency modulation caused by large-scale integration of new energy [5]. How to enhance the active frequency regulation support on the power generation side of the new power system has become a hot topic [6]. To this end, the Shanxi Energy Regulatory Office issued a letter to solicit opinions on the 'Real-time Rules for Shanxi Independent Energy Storage Power Stations to Participate in the Primary Frequency Regulation Market Transaction (Trial)', to provide policy assistance for encouraging market players to actively participate in the primary frequency regulation market, and to clearly encourage and drive new energy storage technology as an independent market subject to participate in various types of electricity markets, such as the spot market and the 'pay-for-effect' ancillary service market.

The hybrid energy storage system (HESS) can combine the advantages of different types of energy storage technologies and provide strong adjustment capabilities

for power balance at different time scales and operating states [7]. Meanwhile, as an effective means to solve the problem of grid-connected clean energy, it has attracted a lot of attention in the field of primary FM by virtue of the advantages of accurate tracking, fast response speed, high control accuracy, and bidirectional regulation capability. However, how to mobilise the enthusiasm and initiative of the energy storage system to participate in frequency modulation, and how to realise the optimal configuration of the hybrid energy storage capacity has become the key to the new power system [8].

Cao *et al.* [9] proposed a coordinated primary frequency regulation control strategy based on multi-objective optimisation. Based on the regional control error of historical typical days, Zhao *et al.* [10] established an optimal configuration model of frequency modulation energy storage capacity based on ensemble empirical mode decomposition method. Jia *et al.* [11] proposed a strategy of primary frequency regulation combined with wind power and energy storage, which made the wind farm have the ability of primary frequency regulation similar to that of traditional power supply. Miao *et al.* [12] proposed a method of smoothing wind power fluctuation based on improved moving average filtering and ensemble empirical mode decomposition. Cheng *et al.* [13] proposed a wind power grid-connected control strategy of HESS based on adaptive moving average algorithm and genetic algorithm-variational mode decomposition (GA-VMD). Lai *et al.* [14] proposed a joint optimisation method for capacity configuration and control strategy of HESS. Jiang *et al.* [15] proposed a hybrid energy storage power allocation strategy based on adaptive moving average algorithm and GA-VMD. Aiming at the problem of deep charging and discharging of hybrid energy storage caused by the common power allocation strategy, Yan *et al.* [16] proposed a two-layer energy management structure considering the optimisation and coordinated scheduling of the state of charge (SOC) of hybrid energy storage. Aiming at the difficulty of power supply in remote areas, Yang *et al.* [17] proposed an optimal configuration method of hybrid energy storage microgrid considering battery life. Aiming at the lowest annual investment cost and daily operation cost, a bi-level optimal configuration model of microgrid was established, and the original problem was transformed into a mixed integer linear programming problem by linearisation method. Xue *et al.* [18] proposed a wind-storage combined frequency modulation control strategy to avoid secondary frequency drop in multiple time scales. Yang *et al.* [19] proposed a method to estimate the optimal battery capacity based on the statistical characteristics of wind farm power (including long-term average and standard deviation).

However, the existing literature mainly focuses on the unilateral research on the control strategy of a wind-storage collaborative system or the capacity configuration of a HESS, ignoring the primary frequency regulation auxiliary service function of the combination of a new energy station and a hybrid energy storage capacity configuration. Therefore, this paper aims at wind farm hybrid energy storage to meet the output requirements

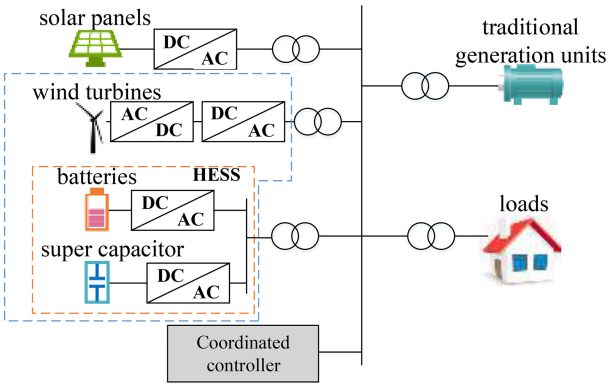

Figure 1. Microgrid power generation system structure.

of the primary frequency modulation of the wind farm in the power system. The VMD is used to decompose the power difference of the primary frequency modulation of the wind turbine. At the same time, the artificial fish swarm algorithm with an improved moving strategy is used to realise the optimal separation of the intrinsic mode components of the VMD so as to determine the optimal capacity allocation of the hybrid energy storage. Because hybrid energy storage has many benefits that work well together, it can help improve the active frequency modulation support goal of the power generation side of the new power system.

2. Microgrid Power Generation System

2.1 System Structure

The microgrid power generation system includes four parts: power generation system, energy storage system, load, and controller [20], and its structure is shown in Fig. 1. Wind-photovoltaic (PV) power systems in microgrids are systems that convert wind and sunlight resources into high-grade electrical energy, respectively, and store the energy in batteries. During the day, when the light intensity increases dramatically, if the power generated is greater than the power consumed by the load, the excess solar energy is selected to be stored in the hybrid storage system for use during peak hours. The system consists of three parts: energy generation, energy storage, and energy consumption. The energy generation part is divided into wind power and PV power generation. For the design of a wind-PV power system, there are two main methods for power determination: one is the power matching method, *i.e.*, the power of the corresponding PV array and the power of the wind turbine are greater than the power of the load under different radiation and wind speeds, which is mainly used for the optimisation and control of the system, and the other is the energy matching method, where the power generation of the corresponding PV array and the power generation of the wind turbine are greater than or equal to the power consumption of the load under different radiation and wind speeds, which is mainly used for the design of the system power. Power consumption of the load, which is mainly used for system power design.

The controller controls the HESS to participate in the primary frequency regulation of the system through energy management distribution, reduces system volatility, and ensures the reliability of the user load power supply [21].

2.2 Variational Mode Decomposition

In this paper, the VMD-Hilbert method is used to decompose the HESS reference power signal. The decomposed signal is called the intrinsic mode function (IMF) of the original signal. The IMF component is reconstructed to construct a new time-space filter to obtain the initial power allocation of HESS. The specific principle equation involving VMD is as follows:

1) The reference power signal $x(t)$ is expressed as:

$$x(t) = \sum_{k=1}^{K} u_k(t) \tag{1}$$

In the formula: K is the decomposition scale.$u_k(t)$ is the corresponding modal components.

2) The Hilbert transform is expressed as:

$$H[u_k(t)] = \frac{1}{\pi} \int_{-\infty}^{+\infty} \frac{u_k(\tau)}{t-\tau} \mathrm{d}\tau \tag{2}$$

3) Converted into polar coordinate form is:

$$z_k(t) = u_k(t) + jH[u_k(t)] = a_k(t) e^{[j\phi_k(t)]} \tag{3}$$

In the formula: a_k is the amplitude value function. $\phi_k(t)$ is the phase contrast electronic microscope function.

$$\phi_k(t) = \arctan \frac{H[u_k(t)]}{u_k(t)} \tag{4}$$

Where the instantaneous power of $u_k(t)$ is:

$$w_k(t) = \frac{d\phi_k(t)}{dt} \tag{5}$$

Where, $w_k(t)$ is the instantaneous power of $u_k(t)$ and can be called the IMF centre frequency.

The resulting Hilbert amplitude spectrum is:

$$H(w,t) = \mathrm{Re}\left[\sum_{k=1}^{K} a_k(t) \exp\left(j \int \mathrm{wk}(t)\, dt\right)\right] \tag{6}$$

4) The Hilbert marginal spectrum obtained by integral is:

$$h(w,t) = \int_{-\infty}^{+\infty} H(w,t) dt \tag{7}$$

5) Finally, the target power of the supercapacitor and the lithium battery in the HESS is obtained:

$$\begin{cases} P_{sc0}(t) = \sum_{k=a+b+1}^{K} u_k(t) \\ P_{Li0}(t) = \sum_{k=a+b+1}^{K} u_k(t) \end{cases} \tag{8}$$

Where, a and b are the frequency filtering order, a smaller, low-frequency part contains more components, the need to configure the lithium battery capacity is larger. Selected b is larger, the higher frequency component will be more, need to configure the capacity of the supercapacitor will be larger.

3. The Objective Function of the Optimal Configuration Model of Primary Frequency Regulation Capacity of Wind Storage

3.1 The Output Required for Primary Frequency Regulation

Aiming at the output required for new energy stations to participate in primary frequency regulation, combined with the 'Technical Specification for Power System Network Source Coordination DLT1870-2018' document issued by the National Energy Administration, the mathematical expression of the output required for primary frequency regulation is as follows:

$$P_n = P_0 - \frac{1}{\delta\%} \times P_N \times \frac{\Delta f}{f_N} \tag{9}$$

Where, P_n is the new energy field station to participate in a frequency regulation in the required power changes. P_0 is the new energy field station initial power. $\delta\%$ is the wind power station frequency regulation difference rate. P_N is the new energy field station rated power. Δf is the frequency difference. f_N is the power grid rated frequency 50 HZ.

$$\begin{cases} \forall f_A \in [0, f_N - f_d], \Delta f = f_A - f_N + f_d, \Delta f \in [-0.1, 0] \\ \forall f_A \in [f_N - f_d, f_N + f_d], \Delta f = 0 \\ \forall f_A \in [f_N - f_d, +\infty], \Delta f = f_A - f_N - f_d, \Delta f \in [0, 0.1] \end{cases} \tag{10}$$

Where, f_A is the actual frequency of the grid, for the dead zone of the primary frequency regulation. f_d is the frequency fluctuation data of the grid operation into this formula, you can find different moments of energy storage system required power.

3.2 Objective Function

Aiming at the lowest cost of HESS when meeting the requirements of primary frequency regulation output of wind farms. It is expressed as:

$$C_1 = \min\{C_B + C_C + C_D\} \tag{11}$$

Where,

$$C_B = \frac{\lambda(1+\lambda)^{Y_B}}{(1+\lambda)^{Y_B} - 1} k_{\mathrm{DE}} (k_{BP} P_B + k_{\mathrm{BE}} E_B + k_{\mathrm{BY}} E_B) \tag{12}$$

$$C_C = \frac{\lambda(1+\lambda)^{Y_C}}{(1+\lambda)^{Y_C} - 1} k_{\mathrm{DE}} (k_{\mathrm{CP}} P_C + k_{\mathrm{CE}} E_C + k_{\mathrm{CY}} E_C) \tag{13}$$

$$k_{\mathrm{DE}} = \frac{1}{T} \tag{14}$$

$$C_D = k_{\mathrm{BE}} E_B + k_{BP} P_B + k_{\mathrm{CE}} E_C + k_{\mathrm{CP}} P_C \tag{15}$$

In (5)–(8): C_1 is the comprehensive cost of HESS primary frequency modulation (converted to equal annual value), MW. C_B is the operation cost of lithium battery, \$/MW. C_C is the operating cost of supercapacitors, MW. C_D is the investment cost of HESS, \$/MW. λ is the discount rate, %. Y_B is the service life of lithium battery, *a*. Y_C is the service life of the supercapacitor, *a*. k_{BP}, k_{BE}, k_{BY} are the unit power cost, unit capacity cost, operation and maintenance cost of lithium battery, respectively, \$/MW; k_{CP}, k_{CE}, k_{CY}, k_{DE} are the unit power cost \$/MW, unit capacity cost \$/MW, operation, and maintenance cost \$/MW, and depreciation coefficient of supercapacitors \$/a, respectively; P_B is the rated power of the lithium battery, MW; E_B is the rated capacity of lithium battery, MW; P_C is the rated power of the supercapacitor, MW; E_C is the rated capacity of the supercapacitor, MW; T is the design replacement period of the equipment, *a*.

3.3 Constraint Conditions

The constraints followed for the composition of the components of the HESS in this paper are mainly borrowed from references [17]–[20], on the basis of which improvements are made to meet the needs of this paper.

1) HESS residual capacity constraint

The normal operation state of the energy storage system is closely related to the service life. To prolong the service life of the energy storage system, it is necessary to ensure that the remaining capacity meets the following constraints at any time:

$$\begin{cases} E_B(t) = E_B(t-\Delta t) - P_B(t)\Delta t\eta_B, (P_B(t) < 0) \\ E_B(t) = E_B(t-\Delta t) - \frac{P_B(t)\Delta t}{\eta_B}, (P_B(t) \geq 0) \\ E_{\mathrm{Bmin}} \leq E_B(t) \leq E_{\mathrm{Bmax}} \end{cases} \tag{16}$$

$$\begin{cases} E_C(t) = E_C(t-\Delta t) - P_C(t)\Delta t\eta_C, (P_C(t) < 0) \\ E_C(t) = E_C(t-\Delta t) - \frac{P_C(t)\Delta t}{\eta_C}, (P_C(t) \geq 0) \\ E_{\mathrm{Cmin}} \leq E_C(t) \leq E_{\mathrm{Cmax}} \end{cases} \tag{17}$$

In the formula, $E_B(t)$, $E_C(t)$ are the residual capacity of lithium battery and supercapacitor at the moment t, respectively, MW. $E_B(t-\Delta t)$, $E_C(t-\Delta t)$ are the remaining capacity of lithium battery and supercapacitor at the moment $t-\Delta t$, MW. E_{Bmax}, E_{Cmax} are the upper limits of the remaining capacity of lithium batteries and supercapacitors in HESS, respectively, MW. $P_B(t)$, $P_C(t)$ are the actual charging and discharging power of lithium battery and supercapacitor at the moment t (positive when discharging and negative when charging), MW. η_B, η_C are the charge and discharge efficiency of lithium battery and supercapacitor, respectively, %. Δt is the calculation of the step size, the step size is too large may lead to the optimisation algorithm cannot converge, the step size is too small will lead to the optimisation algorithm convergence is very slow, increasing the time to find the optimal solution, this paper draws on reference [22] decided to set to 1 min.

The initial and final storage capacity of each research cycle needs to be consistent to ensure the continuity and periodicity of the operation of the HESS, that is:

$$\begin{cases} E_B(T) = E_B(0) \\ E_C(T) = E_C(0) \end{cases} \tag{18}$$

In the formula, $E_B(0)$, $E_C(0)$ are, respectively, the initial capacity of lithium batteries and supercapacitors in HESS, MW.

2) Charging and discharging power constraint

To realise that the battery energy storage system can continue to participate in frequency modulation, this paper manages the SOC of each battery pack in the energy storage station in real time and suppresses the deep charge and deep discharge of each energy storage unit. The HESS charge and discharge power constraint at the moment is expressed as:

$$\begin{cases} P_{\mathrm{Bmin}} \leq P_B(t) \leq P_{\mathrm{Bmax}} \\ P_{\mathrm{Cmin}} \leq P_C(t) \leq P_{\mathrm{Cmax}} \end{cases} \tag{19}$$

When the remaining capacity of HESS cannot guarantee the required charging power, the discharge power of HESS needs to be adjusted, which is expressed as follows:

$$\begin{cases} P_B(t) = \max\left\{P_{B0}(t), \frac{(E_B(t-\Delta t)) - E_{\mathrm{Bmax}}}{\Delta t\eta_B}\right\} \\ P_C(t) = \max\left\{P_{C0}(t), \frac{(E_C(t-\Delta t)) - E_{\mathrm{Cmax}}}{\Delta t\eta_C}\right\} \end{cases} \tag{20}$$

When the remaining capacity of HESS cannot guarantee the required discharge power, the discharge power of HESS needs to be adjusted, which is expressed as follows:

$$\begin{cases} P_B(t) = \min\left\{P_{B0}(t), \frac{(E_B(t-\Delta t)) - E_{\mathrm{Bmin}}}{\Delta t\eta_B}\right\} \\ P_C(t) = \min\left\{P_{C0}(t), \frac{(E_C(t-\Delta t)) - E_{\mathrm{Cmin}}}{\Delta t\eta_C}\right\} \end{cases} \tag{21}$$

3) Energy deviation constraint

$$R = \sqrt{\frac{\sum_{i=1}^{T}\left(P_A(t) - P_{A0}(t)\right)^2}{T-1}} \leq R_{\max} \tag{22}$$

In the formula: $P_{A0}(t)$ is the power of the tie-line protocol, MW. $R_{\max}$ is the maximum root mean square deviation value.

4) Pitch angle variation constraint of wind turbine

When the wind turbine is running, the pitch angle is specified between 0–30° [16].

3.4 Artificial Fish Swarm Algorithm to Optimise the Hybrid Energy Storage Capacity

The artificial fish swarm algorithm is an optimisation algorithm proposed by imitating a series of behaviours of fish foraging [23]. The characteristics are expressed as follows: $X_v = X + \mathrm{Visual} * \mathrm{Rand}()$, $X_{\mathrm{next}} = X + \frac{X_v - X}{\|X_v - X\|} * \mathrm{Step} * \mathrm{Rand}()$.

Among them, Rand() is the random function; Step which is the step size.

However, the setting of sight distance and step length in the algorithm will affect the results of the fish swarm search. Therefore, the improved sight distance and step size set in this paper according to reference [24] are:

$$\text{Visual}_{(0)} = 0.2 \times \sqrt{\begin{array}{l}(E(t)_{\max} - E(t)_{\min})^2 \\ \quad + (C_1(t)_{\max} - C_1(t)_{\min})^2\end{array}} \quad (23)$$

$$\text{Step}_{(0)} = 0.1 \times \text{Visual}_{(0)} \quad (24)$$

The formula, $\text{Visual}_{(0)}$ and $\text{Step}_{(0)}$ represent the sight distance and step of artificial fish. $E(t)_{\max}$ and $E(t)_{\min}$, respectively, represent the maximum and minimum values of the hybrid energy storage capacity to be planned at the moment. $C_1(t)_{\max}$ and $C_1(t)_{\min}$ represent the maximum and minimum values of the frequency modulation cost of the hybrid energy storage at the moment are represented, respectively.

The specific solution process is as follows:

1) Read the primary frequency modulation power difference data and system parameters
2) The total power $P_{\text{HESS}}(t)$ of HESS is obtained by using (9)
3) According to the characteristics of each energy storage in HESS, VMD is used to reconstruct the total power of hybrid energy storage with high and low frequency by using (1)–(8)
4) Data initialisation
5) Calculate the initial sight distance $\text{Visual}_{(0)}$ and step length $\text{Step}_{(0)}$
6) Updating the improved sight distance and step length
7) Judge whether the value obtained by continuous multiple times meets the requirement of primary frequency regulation output
8) If satisfied, the output lithium battery capacity value and supercapacitor capacity value; otherwise, return to step 5
9) The different objective functions E_B and E_C are solved, respectively, to determine whether the constraints are satisfied
10) Repeat the above steps to obtain the final lithium battery capacity E_B and supercapacitor capacity E_C.

4. Example Analysis

4.1 Model Parameters

This paper uses the historical wind farm data of a certain area in Shanxi Province. The relevant system parameters are set in Table 1. When the wind turbine is below the rated wind speed, the pitch control mechanism is not triggered and the pitch angle of the wind turbine blades is 0°, so the aerodynamic thrust increases as the wind speed increases. When equal to and higher than the rated wind speed, the pitch controller operates to regulate the aerodynamic torque of the wind turbine by changing the pitch angle of the blades, and performs load shedding operation when the maximum requirement of the pitch angle is reached. In this paper, the overall technical parameters of the wind turbine

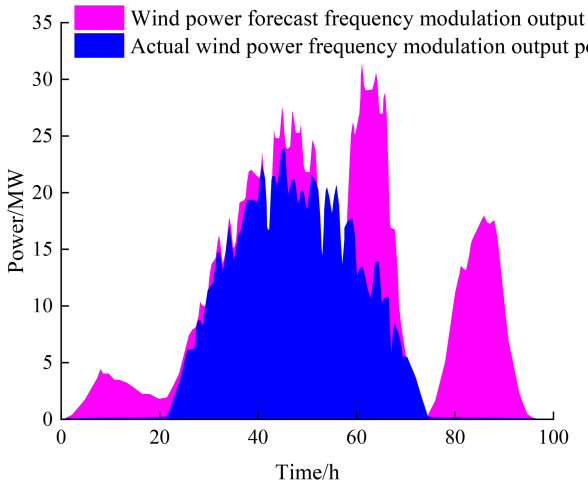

Figure 2. Predicted output of wind turbine.

of Sinovel Wind Energy Co., Ltd. in 2012 are taken as an example to select the appropriate wind turbine parameters.

4.2 Wind Power Frequency Regulation Output Prediction

VMD is used to decompose the fluctuation power required by the HESS. To verify the effectiveness of VMD decomposition power, the historical operation scenario data when the primary frequency regulation of the power grid is insufficient is counted and reduced to a typical scenario, and the original output of the wind farm within 96 h is obtained. At the same time combined with the (9) to get the wind power primary frequency predicted output value, as shown in Fig. 2, due to the impact of the wind farm's own interests, will not be selected in the system needs to be a time when the frequency transmission increase operation, because if this operation will cause the wind farm the actual transmission increase, the wind turbine operation to increase the cost is much greater than the profit gained from the sale of electricity, thus resulting in the wind power of the actual frequency output and the prediction of certain difference. This paper is based on this experimental simulation analysis. The sampling data time is 96 h, the sampling interval is 1 h. The next whole once the frequency experiment is based on this scene above the calculation and analysis.

4.3 HESS FM Power Decomposition

At this time, the original output power of wind power is insufficient, and the output power of the wind farm needs to be adjusted to meet the demand of predicted frequency modulation output. At the same time, HESS was introduced to enhance the stability of wind farm side output. Combined with AFSA and VMD, the frequency fluctuation of power grid lines is deeply decomposed and studied, and the hybrid energy storage is obtained to stabilise the frequency target fluctuation within 96 h of the line, as shown in Fig. 3. The adaptive modal decomposition of the total power of the hybrid energy storage in Fig. 3 is

Table 1
Model Parameters

Object	Parameter	Numerical value
Wind turbine	Pitch angle range/°	[0, 30]
	Speed range/p.u	[0.7,1.2]
	Output power range under wind speed range of 3–5 m/s/ p.u	[0,0.81]
	Output power range under wind speed range of 5.5–9.5 m/s/ p.u	1.2
	Wind speed range of 10–10.5 m/s and above wind speed output power range/ p.u	1.2
Lithium battery	Unit power cost k_{BP}/(\$/MW)	46×10^4
	Unit capacity cost k_{BE}/(\$/MW)	15.5×10^4
	Running-maintenance cost k_{BY}/(\$/MWh)	0.005×10^4
	Charge-discharge efficiency η_B/%	90
	Initial capacity $E_{B(0)}$/MWh	$0.5E_B$
	The upper limit of remaining capacity $E_{B\max}$/MWh	$0.8E_B$
	The lower limit of residual capacity $E_{B\min}$/MWh	$0.2E_B$
	Running time/h	96
Supercapacitor	Unit power cost k_{SCP}/(\$/MW)	21.5×10^4
	Unit capacity cost k_{SCE}/(\$/MW)	82.04×10^4
	Running-maintenance cost k_{SCY}/(\$/MWh)	0.005×10^4
	Charge-discharge efficiency η_C/%	95
	Initial capacity $E_{C(0)}$/MWh	$0.5E_C$
	The upper limit of remaining capacity $E_{C\max}$/MWh	$0.9E_C$
	The lower limit of residual capacity $E_{C\min}$/MWh	$0.1E_C$
	Running time /a	10
Miscellaneous	Discount rate λ/%	6
	Maximum energy root mean square deviation $R_{\max}$	0.1
	Upper and lower limits of primary frequency modulation dead zone	±0.033 HZ
	Upper and lower limits of primary frequency modulation dead zone m/s	[0, 20]

performed, and the results are shown in Fig. 4. A total of 10 components, IMF1∼IMF9 is the inherent mode of the total power of hybrid energy storage, and r9 is the signal trend term. With the increase of modal component order, the frequency variation of each mode decreases gradually. The population number of the multi-objective optimization algorithm in this paper is 500, the number of iterations is 50, and the iterative solution process is shown in Fig. 5. According to (4)–(10), the total power of hybrid energy storage is reconstructed. IMF1∼IMF2 is selected as the supercapacitor power instruction, and IMF3∼IMF9 and its remainder are the hybrid energy storage power instruction, as shown in Fig. 6.

From Fig. 6, it can be seen that the signal frequency processed during VMD signal decomposition has a smaller amplitude difference with the original signal, 1 which is closer to the original wind power output curve, and at the same time, it plays a better smoothing role in the frequency peaks and valleys, and it can more accurately assign the band-decomposition signals to the HESS, so

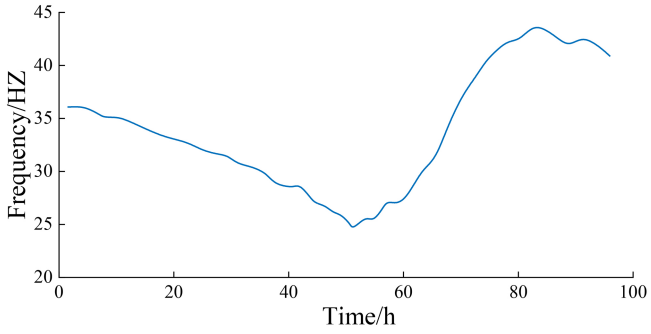

Figure 3. Frequency fluctuation of the line within 96 h.

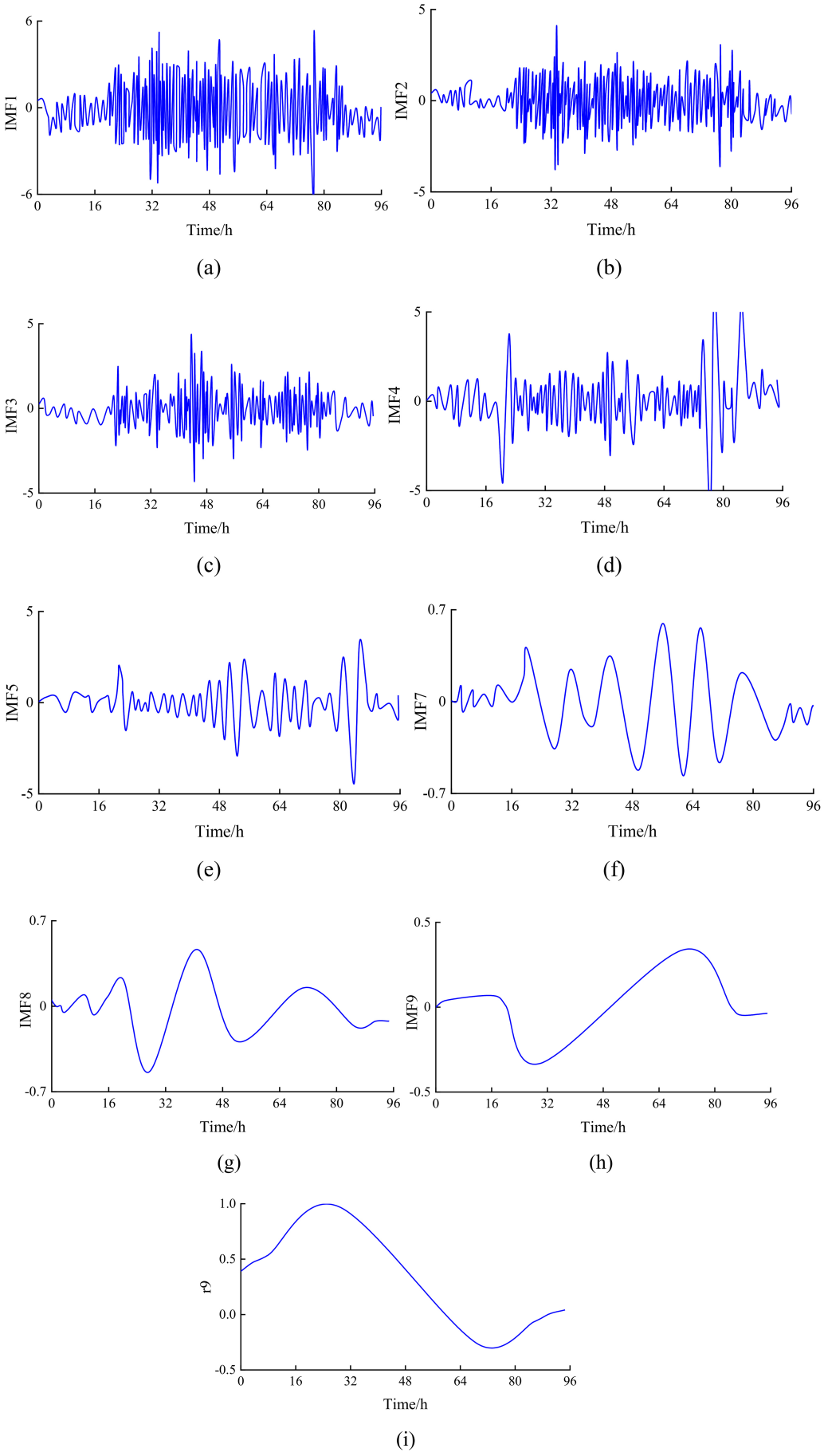

Figure 4. VMD decomposition results.

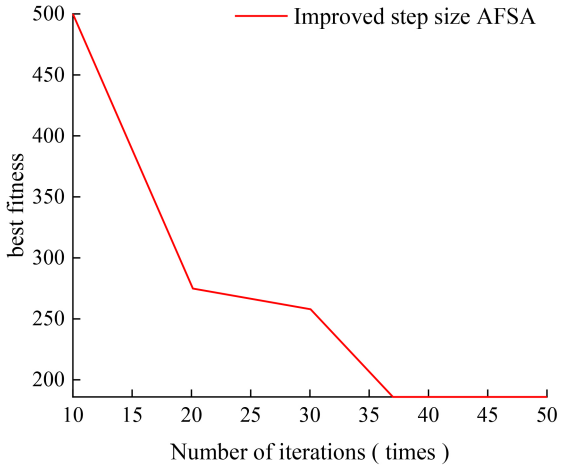

Figure 5. AFSA optimisation process.

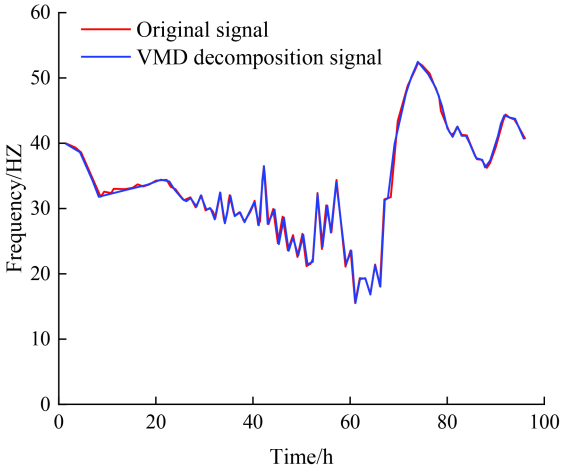

Figure 6. VMD signal decomposition and original signal comparison diagram.

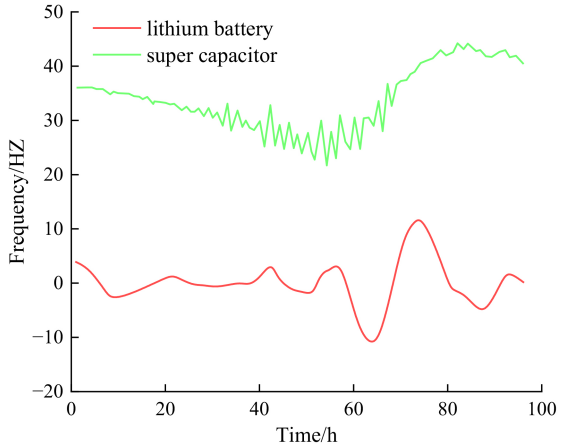

Figure 7. HESS output strategy diagram.

that the HESS is more smoothly and accurately during the one-time frequency modulation output of the auxiliary wind farm. The HESS power output strategy based on VMD decomposition is shown in Fig. 7. During the primary frequency modulation of the wind farm, the Li-ion battery

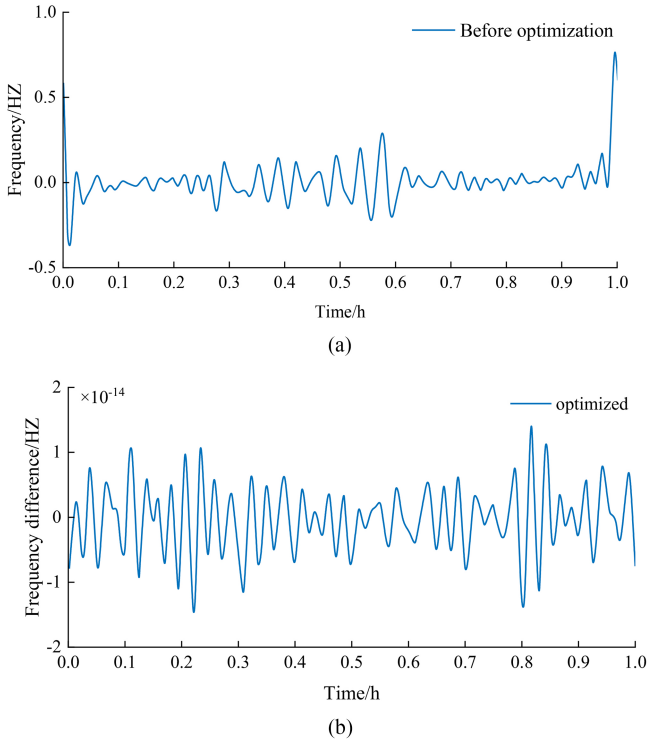

Figure 8. Comparison before and after frequency optimisation.

pack is mainly responsible for the output stabilisation of the high-frequency part of the signal, and the SC is mainly responsible for the throughput stabilisation of the low-frequency signal. This allocation strategy takes into account the loss cost of lithium battery during deep charging and discharging transformations and the stable output characteristics of lithium battery compared with SC, avoiding excessive loss of lithium battery caused by a frequency modulation and a substantial increase in loss cost.

The frequency fluctuation changes before and after optimisation in 1 h within 59–60 h are compared. The comparison before and after frequency optimisation is shown in Fig. 8. It can be seen that the line frequency fluctuation has been significantly improved after the introduction of HESS. Through the reasonable decomposition of the target frequency by VMD, the decomposed power fluctuation is controlled in a very small range, which enhances the fineness of the HESS capacity optimisation configuration stage.

During the whole primary frequency modulation period, the output of HESS is shown in Fig. 9. SC is mainly responsible for the low-frequency part with many frequency conversion times. As a power-type energy storage battery, SC has the characteristics of fast response time, short response time, and frequent charge and discharge, reducing the deep charge and deep discharge of lithium battery packs to extend the service life of the battery energy storage system. The lithium battery pack is mainly responsible for supplementing the frequency difference and maintaining the stable output of the frequency modulation power for a long time.

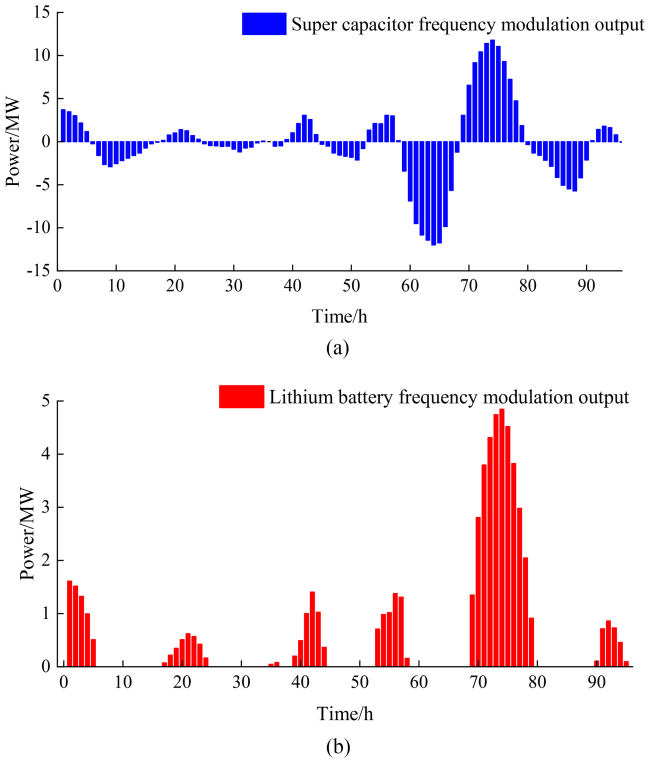

Figure 9. HESS diagram.

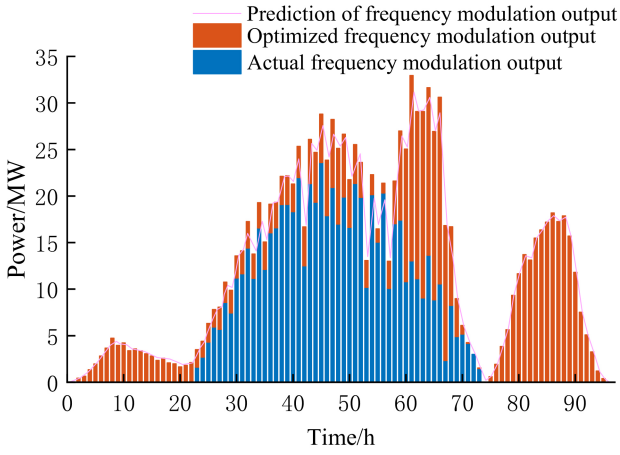

Figure 10. Wind power frequency regulation adjustment output diagram.

With the help of HESS, the output of wind power frequency regulation is shown in Fig. 10. The VMD signal decomposition accurately allocates the target power to HESS and wind turbines. At this time, the wind turbines and HESS can be regarded as an income whole, avoiding the wind turbines giving up participating in the frequency modulation work due to the high start-stop cost in the period of low demand for wind power frequency modulation. The overall transmission of frequency modulation power from the wind farm to the external network is shown in Fig. 11. The cooperation of wind turbines and HESS can meet the demand for primary frequency regulation of wind farms. At the same

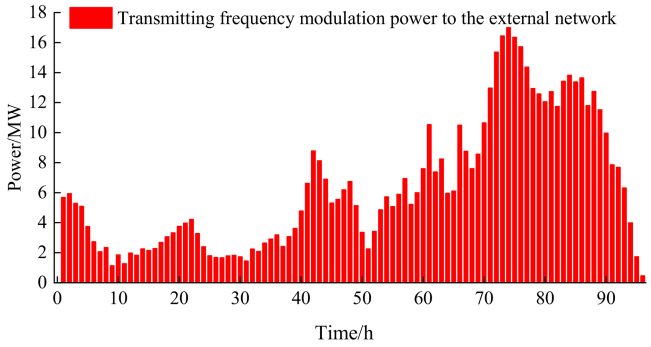

Figure 11. Frequency modulation power transmitted by external network.

Table 2
Wind Farm HESS Configuration Results

Storage mode	Capacity allocation/WM	Cost/$
SC	12.71	816.81×10^4
Lithium battery pack	49.28	847.91×10^4

time, because HESS itself has the characteristics of "high-low charge", this characteristic can be used to reserve the excess frequency regulation power generation of wind turbines and release it during the peak period of electricity consumption, which not only plays the role of "peak shaving and valley filling" but also brings additional income to wind farms. The wind farm HESS configuration results and the additional frequency modulation power sold by the wind farm after the AFSA solution are shown in Table 2. By selling the remaining frequency modulation power stored in HESS, wind farms can achieve a certain amount of additional economic income.

5. Conclusion

With the increasing number of new energy power generation devices connected to the grid year by year, its variability and volatility bring great hidden dangers to the safe operation of the power grid. In this paper, aiming at the problem of how to change the primary frequency regulation of wind power generation from 'intermittent' to 'reliable', combined with the 'Power System Network Source Coordination Technical Specification DLT1870-2018' document, from the perspective of a wind farm, a hybrid energy storage capacity optimisation configuration research method considering primary frequency regulation auxiliary services is proposed. The conclusions are as follows:

(1) The combination of AFSA and VMD optimises the HESS system and size. AFSA chooses the appropriate frequency component. Then, the VMD with the determined frequency component is used to decompose the primary frequency modulation target power. The lithium battery and the super capacitor, respectively, are responsible for bearing the high- and

low-frequency target power after decomposition. This method can improve the power efficiency of HESS decomposition, and the capacity configuration is more reasonable. At the same time, the remaining power stored in HESS can be sold through the power frequency regulation auxiliary market to obtain a certain economic return, improve the efficiency of wind farms, and enhance the initiative of primary frequency regulation of wind farms.

(2) This method reduces the problem of unstable frequency regulation output in wind farms and enhances the stability of the primary frequency regulation output of wind turbines.

Acknowledgement

The study received no funding.

References

[1] Y.B. Shu, Z.G. Zhang, J.B. Guo, and Z.L. Zhang, Research on key factors and solutions of new energy consumption, *Chinese Journal of Electrical Engineering, 37*(1), 2017, 1–9.

[2] J.H. Li, J.H. Zhang, G. Mu, *et al.*, Day-ahead optimal scheduling strategy for energy storage peak shaving considering load peak-valley characteristics, *Power Automation Equipment, 40*(7), 2020, 128–133.

[3] Z.G. Zhang and C.Q. Kang, Challenges and prospects of building a new power system under the goal of carbon neutrality, *Chinese Journal of Electrical Engineering, 42*(8), 2022, 2806–2819.

[4] F. Arrigo, E. Bompard, M. Merlo, and *F.* Milano, Assessment of primary frequency control through battery energy storage systems, *International Journal of Electrical Power & Energy Systems, 115*, 2020, 105428.

[5] Z.X. Tan, X.R. Li, L. He, Y. *Li*, and J.Y. Huang, Primary frequency control with BESS considering adaptive SoC recovery, *International Journal of Electrical Power & Energy Systems, 117*, 2020, 105588.

[6] B. Liu, J. Zhang, D.X. Li, and N. Ning, Energy storage for peak shaving and frequency regulation in the front of meter: Progress and prospect, *Energy Storage Science and Technology, 5*(6), 2016, 909–914.

[7] A. Mamun, Z. Liu, D. Rizzo, and S. Onori, An integrated design and control optimization framework for hybrid military vehicle using lithium-ion battery and supercapacitor as energy storage devices, *IEEE Transactions on Transportation Electrification, 5*(1), 2019, 239–251.

[8] Q.Y. Lu, Y.G. Yang, and P.P. Xie, Market mechanism design and scheduling strategy of frequency modulation auxiliary service adapted to energy storage participation, *Grid Technology*, 2023. DOI: 10.13335/j.1000-3673.pst.2022.2166.

[9] Y.J. Cao, Q.W. Wu, and H.X. Zhang, Optimal sizing of hybrid energy storage system considering power smoothing and transient frequency regulation, *Electrical Power and Energy Systems, 142*(Part A), 2022, 108227.

[10] X.L. Zhao, P. Li, and B. Fu, Control strategy of wind-storage coordinated primary frequency regulation based on multi-objective optimization, *China Southern Power Grid Technology, 16*(10), 2022, 68–76.

[11] Y.B. Jia, J. Zheng, H. Chen, *et al.*, Optimal allocation of energy storage capacity based on ensemble empirical mode decomposition, *Power Grid Technology, 42*(9), 2018, 2930–2937.

[12] F.F. Miao, X.S. Tang, and Z.P. Qi, Energy storage participating in capacity optimization of wind power primary frequency modulation, *New Technology of Electrical Engineering, 35*(4), 2016, 23–29.

[13] Y.M. Cheng, G.J. Meng, P. Jia, *et al.*, Hybrid energy storage capacity optimization for wind power fluctuation, *Journal of Power Sources*, 2023.

[14] J.J. Lai, X.L. Wen, and Q. Zhang, Hierarchical coordination control strategy for wind-storage-DC microgrid, *Journal of Wuhan Institute of Technology, 44*(6), 2022, 675–682.

[15] F. Jiang, T.L. Xue, L. Zhang, *et al.*, Power distribution strategy of hybrid energy storage to smooth wind power fluctuation, *Northeast Electric Power Technology, 43*(10), 2022, 49–55.

[16] N. Yan, S. Guo, and J.G. Shi, Optimal configuration and control strategy of hybrid energy storage for wind power fluctuation reduction, *Electrical Engineering*, (18), 2022, 44–50.

[17] X.H. Yang, Z.X. Yuan, J.Y. Xiao, *et al.*, Optimal configuration of hybrid energy storage microgrid considering battery life, *Power System Protection and Control, 51*(4), 2023, 22–31.

[18] T.L. Xue, F. Jiang, and L. Zhang, Power distribution and two-layer energy management strategy of mixed energy storage system, *Journal of China Three Gorges University, 45*(1), 2023, 80–87.

[19] S.J. Yang, Optimal allocation of hybrid energy storage capacity based on improved sparrow search algorithm, *Electronic Technology and Software Engineering*, (19), 2022, 134–137.

[20] F.Q. Tang, F. Jun, and J.R. Xie, The control strategy of air storage combined frequency modulation to avoid frequency secondary sag, *Proceedings of the CSEE*, 2023.

[21] T.L. Xue, F. Jiang, L. Zhang, *et al.*, Power distribution and two-layer energy management strategy of mixed energy storage system, *Journal of China Three Gorges University, 45*(1), 2023, 80–87.

[22] L.J. Guo, B. Wei, X.Q. Han, *et al.*, Optimal allocation of hybrid energy storage capacity for AC/DC hybrid microgrids based on ensemble empirical modal decomposition, *High Voltage Technology, 46*(02), 2020, 527–537.

[23] L. Luo, K. Hu, S. Li, *et al.*, Routing algorithm for VANET based on fish swarm optimization, *Journal of University of Electronic Science and Technology of China, 50*(4), 2021, 488–495.

[24] X.M. Liang and J.L., An artificial fish schooling algorithm with improved step size and field of view, *Journal of Beijing Architecture University, 33*(02), 2017, 47–53.

Biographies

Zhiye Lu received the B.Sc. degree in electrical engineering from Northeast Agricultural University, China, in 2021, where he is currently pursuing the M.S. degree in electrical engineering. His current research interests include power quality analysis and control, modeling and operation of microgrid clusters, and optimization of energy storage systems.

Jinze Yu received the B.Sc. degree in electrical engineering from Northeastern Agricultural University, China, in 2022, where he is currently pursuing the M.S. degree in electrical engineering. His research interests include control techniques for dc–dc and ac-ac power converters.

Liyang Sun received the B.Sc. degree in electrical engineering from the HeiLongjiang University, China, in 2019. He is currently pursuing the M.S. degree in electrical engineering with the Northeast Agricultural University, China. His research interests include dc microgrids, smart energy management, and energy storage system.

Yupeng Xiong received the B.Sc. degree in electrical engineering from the Yancheng Institute of Technology, Jiangsu, China, in 2022. He is currently pursuing the M.S. degree in electrical engineering with the Northeast Agricultural University, China. His research interests include wind farms and primary frequency regulation.

Bing Yang received the B.Sc. degree in electrical engineering from Northeast Agricultural University, Heilongjiang, China, in 2022, where he is currently pursuing the M.S. degree in electrical engineering. His research interests include HESS, energy storage system modeling and DC/AC microgrids.

Ruolin Yin received the B.Sc. degree in electrical engineering from Northeast Agricultural University, China, in 2022, where she is currently pursuing the M.S. degree in electrical engineering. Her research interests include integrated data/power coordinated control, and secondary control and optimal operation of DC microgrids.

Lishu Wang received the B.Sc., M.S., and Ph.D. degrees in agricultural electrification and automation from Northeast Agricultural University, Heilongjiang, China, in 1996, 2003, and 2006, respectively. Since 2010, he has been a Professor with the Department of Agricultural Electrification, College of Electricity and Information, Northeast Agricultural University. His research interests in the direction of new energy development and utilization of electric power.